Rodriguez, I.; Fenollosa Esteve, R.; Ramiro Manzano, F.; García-Aboal, R.; Atienzar Corvillo, PE.; Meseguer Rico, FJ. (2019). Groove-assisted solution growth of lead bromide perovskite aligned nanowires: a simple method towards photoluminescent materials with guiding light properties. Materials Chemistry Frontiers. 3(9):1754-1760. https://doi.org/10.1039/c9qm00210c

MATERIALS CHEMITRY FRONTIERS

RESEARCH ARTICLE

Grooves-assisted solution growth of lead bromide Perovskite aligned nanowires: a simple method towards photoluminescent material with guiding light properties

Received 00th ,
Accepted 00th

DOI: 10.1039/x0xx00000x

www.rsc.org/

Isabelle Rodriguez[a], Roberto Fenollosa[a], Fernando Ramiro-Manzano[a], Rocío García-Aboal[a], Pedro Atienzar[a], and Francisco J. Meseguer[a].*

High refractive index nanowires are very attractive because of their waveguiding properties and their multiple applications. In this sense, metal halide Perovskites, an emerging and appealing optoelectronic material, have also been tailored in nanowires structure. Here we present an easy, low-cost and versatile method that has allowed to achieve nanowires of controlled and uniform width. The method has been applied here to all-inorganic and hybrid lead bromide Perovskite ($CsPbBr_3$ and $CH_3NH_3PbBr_3$ respectively) materials. The procedure is based on the spin coating of precursors solutions, at room temperature, on PDMS replica of the periodic grooves and lands of commercially available Compact Disc (CD) or Digital Versatil Disc (DVD) polycarbonate plates. The method can be applied for the synthesis of others material nanowires before being transferred onto other substrates. The obtained $CsPbBr_3$ and $CH_3NH_3PbBr_3$ nanowires exhibit high photoluminescence and guiding light properties along the material.

.

1. Introduction

Nanowire-like nanostructured semiconductors have raised a great interest since they were discovered, two decades ago, as they exhibit unique electrical, and optical properties, making them suitable for applications in optoelectronics, photonic devices or energy generation. [1,2] Particularly, high refractive index nanowires can be used for confining and guiding light at the nano- and micro-scale. That is the reason why they have become elements of paramount importance in photonics, where a technological revolution is expected to happen, similarly to microelectronics in the past century. So far, different base materials have been used to develop nanowires, namely II-VI (ZnO), III-V (GaAs, InP, InSb, GaN, etc) [2], IV (Si, Ge) [3-5] semiconductors, and more recently metal Halide Perovskites could be shaped in nanowire structures. [6,7] That was a very important achievement because metal halide Perovskites (AMX_3) have emerged as an appealing optoelectronic material [8], with a high photoluminescence efficiency [9-13], high optical absorption [14], low charge carrier recombination coupled with high hole and electron mobility [15] that make them very suitable for many optoelectronic applications [16] such as solar cells devices [17-19], light emitting diodes [16,20-22] and optically pumped lasers.[16, 21, 23-25] Moreover, they can be easily synthetized by low-temperature solution processing and the band gap can be tuned through halide substitution or halide mixtures [26] and also by the divalent metal cation replacement. [27] However, in any case, and particularly for Perovskites materials, the shape of the nanowires somehow follows crystalline directions of growth, thus producing nanowires of a given dimension with triangular, or square like shaped cross sections, far from the cylindrical shape of conventional optical fibers. These geometrical parameters play a key role because they determine how light propagates through the nanowire: the losses, and the interaction of light with the nanowire itself and with the surrounding material. Therefore, in spite of the remarkable results obtained so far through chemical vapor deposition [28-37] or via solution phase synthesis [23, 38-51], it is very important to explore new routes that allow tuning the shape and dimensions of 1D Perovskite structures. In this way, recently MAPbX3 nanowires arrays have been grown using PDMS rectangular groove templates obtained from replication of silicon masters previously prepared by photolithography. [52] Herein, we propose, a simple and low-cost method to obtain metal halide Perovskite nanowires based on the confinement of precursor solutions in submicrometer size grooves imprinted on the polycarbonate (PC) sheet of commercial

[a] *Instituto de Tecnología Química (CSIC-UPV), Universitat Politècnica de València, Av. Los Naranjos s/n, 46022 Valencia, Spain*

†Electronic Supplementary Information (ESI) available: Figure S1: FESEM images of DVD substrates and PDMS replica; Figure S2: FESEM images of CD substrates and PDMS replica; Figure S3: $MAPbBr_3$ nanowires characterization: Optical and FESEM images (top and Cross- section view); Figure S4: Experimental optical set-up; Figure S5: $CsPbBr_3$ nanowires grown on PDMS CD-like substrate. PL evolution; Figure S6: PL of $CsPbBr_3$ and $MAPbBr_3$ films; Figure S7: Optical properties of $MAPbBr_3$ nanowires; Figure S8: optical image of $MAPbBr_3$ nanowires transferred onto ITO glass substrate. See DOI: 10.1039/x0xx00000x

recordable DVD or CD plates. Such method of preparation not only allows to obtain nanowires with homogeneous width and shape but also to choose between several width dimensions depending of the employed template. Indeed, as described below, DVD and CD structures can provide plates of different grooves size and distribution.

2. Results and discussion

Recordable DVDs are made of two PC plates patterned with a spiral distribution of grooves and lands, the top one presenting the complementary geometry of the bottom one (See Fig. S1 ESI†). Due to the incompatibility of PC with most of the employed solvents for the synthesis of Perovskites, here, this kind of support cannot be used directly as template. Therefore, patterned Polydimethylsiloxane (PDMS) substrates were prepared via molding procedure of the lands and grooves array of DVD or CD polycarbonate masters. Fig. 1 shows an illustrative general scheme of the preparation and the features of the PDMS templates. The procedure to achieve the corrugated PC substrates is described in the experimental section. The PDMS replica were prepared by pouring the pre-polymer liquid (Sylgard 184 Silicone Elastomer Kit) over the PC plates, and then letting it cure at 60ºC. After mechanically peeling it off from the master, the negative PDMS mold of CD or DVD was obtained (Fig. S2, ESI†). In order to enhance the wettability of the PDMS substrate surface, O_2 plasma treatment was used before the next step. Then, precursor solutions of metal halide Perovskite were drop-casted and spin-coated on the patterned PDMS substrates previously hydrophilized. With an adequate spin speed and time, upon solvent evaporation, nanowires are formed into the grooves of the template. Fig. 2 summarizes the different stages of the procedure. Hence, it can be seen that is a quite low cost and a versatile method that could be used for the preparation of nanowires of any other material from precursors solutions. We have applied this method for synthesizing both hybrid and all-inorganic lead halide perovskite nanowires. The first one, with the general structure $MAPbX_3$ (MA= Methylammonium, X= Cl, Br, I) has been largely studied and their efficiency proved. [18,53] Although some halide derivative seems to show higher stability, a drawback of organic-inorganic halide Perovskites is both, their sensitivity to moisture and O_2 [54,55] as well as their thermal instability [56,57]. Theses disadvantages could be mitigated by the employ of all-inorganic lead halide Perovskites. In this sense, Cesium based lead halide Perovskites seem to combine performance and stability [58-60] and moreover they tend to show a high defect tolerance. [61] Here, $CsPbBr_3$ Perovskite nanowires were synthesized starting from a stoichiometric mixture of dissolution of precursors, CsBr and $PbBr_2$, in Dimethyl Sulfoxide (DMSO).

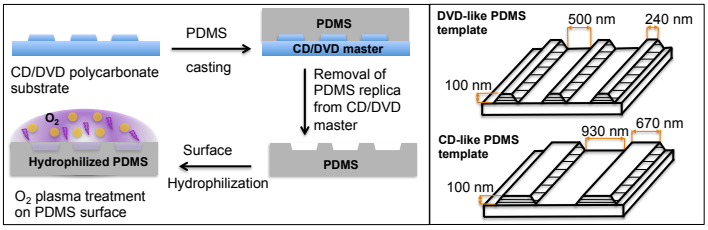

Fig.1: Schematic illustration of the preparation and features of the PDMS template

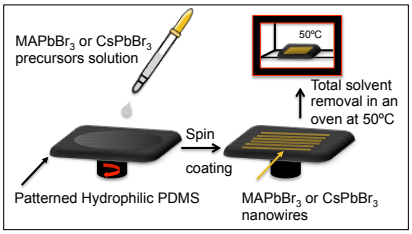

Fig. 2: Preparation procedure of $MAPbBr_3$ and $CsPbBr_3$ nanowires into the grooves of hydrophilized PDMS templates obtained by replication of CD o DVD profiles.

Concerning Methylammonium Lead tribromide ($MAPbBr_3$) nanowires, dissolutions of CH_3NH_2Br and $PbBr_2$ in DMF were employed. A drop of the precursors solution was deposited onto a patterned PDMS stamp (1 cm^2), previously hydrophilized by O_2 plasma treatment. Then the stamp was spin-coated until solvent evaporation and formation of an orange/yellowish material occurred. Finally, the samples were kept at 50º C overnight for a complete removal of any rest of solvent. For the sake of clarity, only results concerning $CsPbBr_3$ material will be shown here (for $MaPbBr_3$ nanowires see supporting information). As it can be seen in the optical and electronic microscopy images in Fig. 3, the growth of $CsPbBr_3$ nanowires takes place into the well-aligned periodic grooves of the PDMS substrates, which correspond to DVD and CD replica patterns.

Precursors solutions fill the grooves of the templates resulting in shape-controlled nanowires upon solvent evaporation. Therefore, the widths are uniform, with values, in the examples shown in fig. 3, of 500 nm and 930 nm for DVD-like and CD-like PDMS templates respectively. Nanowires of several dozen microns of length could be achieved. The cross section area of the obtained nanowires is uniform and it is determined by the size and shape of the patterned grooves in the PDMS template. Fig. 3d and Fig. 3e show Field-Emission Scanning Electronic Microscopy (FESEM) images of a transversal cut of a $CsPbBr_3$ nanowires sample realized by FIB (focused ion beam) milling after sputtered Au or/and Pt coatings to reduce samples charging and beam damage. It can be seen that the material has been conformed to the groove of the template by the spin process to form polycrystalline $CsPbBr_3$ nanowires. A similar behavior is observed for $MAPbBr_3$ material in Fig. S3 (ESI†). Therefore, nanowires features could be tuned by changing the template (and the master) characteristics as well as the precursor solution employed.

The X-ray diffraction (XRD) pattern of the $CsPbBr_3$ nanowires (Fig. 3c) shows 2 strong diffraction peaks with maximum at 2 theta angles of 15.46º and 31º, that match respectively to the (110) and (220) lattice planes of an orthorhombic Perovskite structure obtained at room temperature.[38]

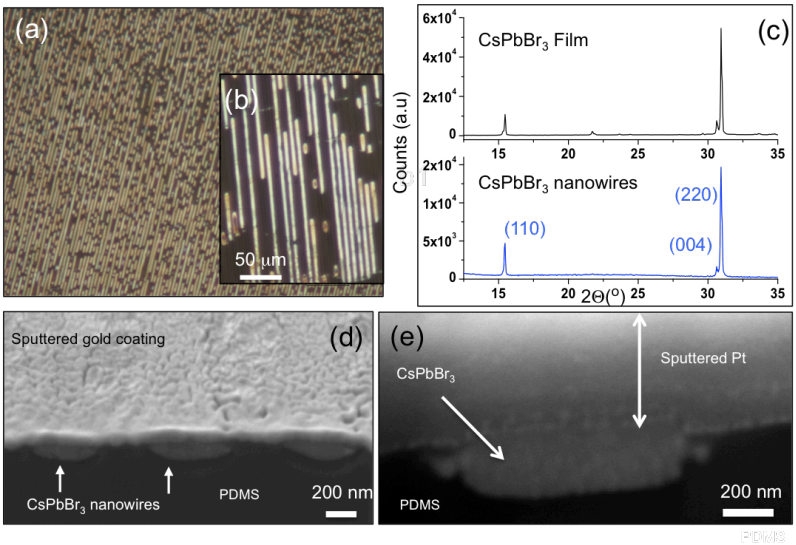

Fig. 3: Polycrystalline $CsPbBr_3$ nanowires characteristics. Optical images of $CsPbBr_3$ Perovskite nanowires obtained on (a) DVD and (b) CD replica PDMS substrates. (c) XRD pattern of $CsPbBr_3$ nanowires and of a $CsPbBr_3$ film structure. (d) FESEM image of a lateral view of a sample of $CsPbBr_3$ nanowires (obtained on PDMS replica of DVD structure) cut by FIB milling perpendicularly to the surface and coated with sputtered gold. (e) FESEM image of the cross section of a $CsPbBr_3$ nanowire grown on PDMS replica of CD structure (Sputtered Pt coating was used to cover the sample before the FIB milling)

In order to confirm the feasibility of the synthesized material to yield photoluminescence (PL) and see if the emitted signal could be guided along the 1D structures, we performed confocal PL spectroscopy on single nanowires and varied the distance between the collection and the excitation points. Specifically, the collection point was fixed at one end of the nanowire so as to acquire the scattered light at that position, while the excitation point was shifted along it. Collection and excitation could be accomplished by using 20 x 0.4 NA objectives in both cases, mounted in forward configuration (Fig. S4 (ESI†)). They allow focusing and collecting light in areas of about 1 or 2 micrometers in diameter. As excitation source we used light of a 405 nm laser, with varying powers around 0.1 mW.

Fig. 4a, 4b, 4c, and 4d show optical microscopy images, recorded by the camera of the set up of Fig. S4 (ESI†), of two neighboring isolated $CsPbBr_3$ nanowires supported on a PDMS replica of a DVD profile substrate (Fig. 3a). For the sake of simplifying the experimental procedure, we chose for the Photoluminescence (PL) measurements the shortest one, which is about 12 μm in length (see the color optical image at the top right of the fig. 4). The images correspond

to different collection-excitation distances ($d_{E\text{-}C}$), which have been indicated under each picture. The white spots on the nanowire correspond to PL signals produced by the excitation laser. The intensities between the images are not comparable due to both camera autofocus and laser intensity adjustment. The bottom end of the nanowire corresponds to the collection point. Therefore, at $d_{E\text{-}C}$ = 0 μm (Fig. 4 a), only one spot appears at that point. The other images, corresponding to $d_{E\text{-}C}$ values different from zero (Fig. 4 b, c, d) show two spots, one coming from the direct excitation of laser upwards and another one, which is less intense, at the collection point. We associated the last signal to that light which is emitted at the excitation point where the laser is focused and travels towards the end of the nanowire, where it is scattered in all directions. Of course, light should travel to the other end of the nanowire as well, but it could not be always recorded by the camera, particularly for long distances from the excitation point. Fig. 4 shows as well the PL spectral evolution (blue, green, black and cyan curves) as a function of the collection-excitation distance ($d_{E\text{-}C}$).

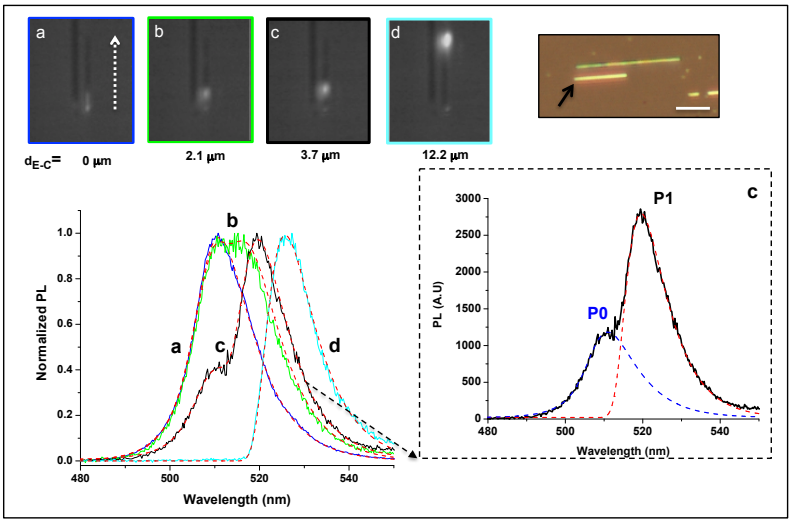

Fig. 4. a, b, c, and d: optical images recorded by the camera of the set up described in Fig. S4 (ESI†) of two neighboring isolated $CsPbBr_3$ Perovskite nanowires obtained into a groove of a DVD based PDMS substrate. The chosen nanowire for PL experiments is indicated by a black arrow in the optical microscopy image at the top right of the figure (scale bar: 10 μm). The white spots on the images (a, b, c, d) correspond to PL signals produced by the excitation laser for several distances, $d_{E\text{-}C}$, specified under each image, between excitation and collection (bottom end of the nanowire) points. The intensities between the images are not comparable because they were recorded with different sensitivity conditions of the camera. Down Left of the figure: The solid color curves correspond to the PL spectra measured for each $d_{E\text{-}C}$ case (same color and label as camera image frames), and the dashed red curves correspond to fits according a theoretical model described in ref. 65. As an example, the plot at the right side shows that the fitted spectrum "c" results from the overlap of two peaks, P0 and P1 (blue and red dashed curves), corresponding respectively to the direct emission of the nanowire and the guided light emission from excitation to collection area.

In general, the intensity of light at the collection point decreases as $d_{E\text{-}C}$ increases as previously reported in others studies [31, 62-64]. Therefore, we adjusted the integration time of the detector and the power of the excitation laser so as to achieve a reliable detection and to obtain a qualitative optical behavior of the material. For this reason and for the sake of comparison, we have normalized all the spectra. At $d_{E\text{-}C}$ = 0 (curve 'a', blue line), a Gaussian like peak with some asymmetry appears with its maximum centered at about 513 nm. As the excitation beam moves away from the collection point, this shape changes substantially. The spectra broaden and new features appear at longer wavelengths. We decomposed each spectrum into two peaks and associated them to two distinct effects by means of a fitting procedure (red dashed curves). Firstly, spectrum 'a' represents the direct-emission of a small portion of the material. The fit of this peak was achieved by using the model described in ref. 65, and assuming a thickness of 106 nm that corresponds to the nanowire height. This permits to obtain the bulk extinction coefficient of the synthetized material. We call this peak as P0. Secondly, the other spectra (b, c, d) include the incoherent addition of P0 with

some attenuation coefficient and another peak, P1 from now on, centered at longer wavelengths. We hypothesize that P1 arises from the guiding phenomenon of light from the excitation to the collection spot. This peak is red-shifted in comparison to P0 because the absorption coefficient is higher for shorter wavelengths within the PL emission of the material. P1 was fitted to the model mentioned above taking into account the $d_{E\text{-}C}$ value for each case. The obtained extinction coefficient from this fit takes, however, a lower effective value than that of the bulk one, regardless of $d_{E\text{-}C}$ and wavelength. We attributed this effect to the guiding mode field profile that probably forces the light to travel partially outside the nanowire core. It can be seen in figure 4 how the fitted spectrum "c" for example can be decomposed into two spectra, P0 and P1.

Finally, we would like to discuss about the presence of P0 at $d_{E\text{-}C}$'s different from zero. Pazos-Outón et *al.*[63] argued in a similar experiment that this kind of effect comes from a photon absorption-reemission phenomenon. However, we think that because the acquired signal is very weak, other effects such as a spurious acquisition of unguided PL from unwanted reflections or spurious excitation by the tail of the laser spot should not be disregarded. In any case, P0 almost disappears for $d_{E\text{-}C}$ > 12 μm. Wider $CsPbBr_3$ nanowires (Fig. 3b and 3e), obtained by using the CD replica as template (Fig. 1, below right) yielded similar results to those of their narrower counterparts (Fig. S5, ESI†). However, the peak P0, that corresponds to the PL at $d_{E\text{-}C}$ = 0 is centered in this case at about a slightly longer wavelength, λ=525 nm, in spite of being the same material.

In fact, the origin of this red shift of the P0 peak comes from a higher thickness of the obtained nanowires and it is in accordance with previous published results.[34] Indeed, from the fit of the spectrum, the thickness of the $CsPbBr_3$ nanowires obtained on PDMS replica of CD substrate is found to be 110 nm. In the same way, photoluminescence of $CsPbBr_3$ and $MAPbBr_3$ film samples is also red shifted in comparison with the nanowires of about 100 nm of thickness. (see Fig. S6, ESI†)

Similar optical studies have been realized on $MAPbBr_3$ Perovskite nanowires and can be seen in supporting information file. (Fig. S7 (ESI†)).

Preliminarily test to transfer nanowires onto other substrates have been performed. Fig. S8 (ESI†) shows an optical image of $MAPbBr_3$ nanowires on ITO glass substrate.

3. Experimental section

DVD and CD polycarbonate substrates. Recordable DVDs are composed of two plates of polycarbonate that were mechanically separated. The bottom one PC sheet is patterned with a spiral periodic distribution of grooves (see Fig S1 of the ESI†) coated with a photosensible dye (where the data can be recorded by a laser beam) and a metallic film. The later one was peeled off by means of an adhesive tape. Then a mixture of water:ethanol (1:1, v/v) was employed to remove the dye coating as described in a previously work [66] The top plate of the DVD presents the complementary profile of the bottom one, providing therefore a Polycarbonate template with wider grooves with less separation between them.

The CD structure is only composed of one plate of polycarbonate patterned with grooves periodically separated (Fig. S2, ESI†) also coated with a dye and a reflective layer that were removed through similar method than the one used for DVD and described above.

PDMS replica molding. Sylgard 184 elastomer kit prepolymer was mixed with the curing agent (10:1 ratio) and degassed under vacuum until removing all air bubbles. The PDMS mixture was then poured on top of the CD or DVD polycarbonate substrates placed in a glass Petri dish. After a curing process of 2h at 60ºC, PDMS layer was mechanically peeled off from the PC plate.

$CsPbBr_3$ and $MAPbBr_3$ precursors solutions preparation. CsBr, MABr, $PbBr_2$, the solvents Dimethylformamide (DMF) and Dimethylsulfoxide (DMSO) were obtained from Sigma-Aldrich. $CsPbBr_3$ precursors solution was prepared by dissolving a stoichiometric mixture of 0.45M CsBr and 0.45M $PbBr_2$ in DMSO prepared at 50ºC. For $MAPbBr_3$ precursors solution, 1M MABr and 1M $PbBr_2$ in DMF was employed and mixed in a 1:1 ratio.[67]

Spin-coating experiments. They were realized on an Ossila spin coater system. Speeds of 2000 rpm (rotation per minute) and of 3000 rpm were used for $MAPbBr_3$ and $CsPbBr_3$ respectively.

Optical and Electronic microscopy. Optical images were taken by a Nikon Eclipse LV100 microscope. Field emission scanning electron microscopy (FESEM) images were obtained on a Carl Zeiss Ultra 55 instrument and the Focused Ion Beam (FIB) milling experiments were performed on a Carl Zeiss AURIGA compact FIB-FESEM workstation.

X-ray Diffraction. X-ray diffraction patterns were recorded on a Bruker D8 Advance A25 X-ray diffractometer operating at 45kV and 80 mA Cu K radiation (= 1.5406Å) equipped with a LYNXEYE XE 1-D detector

Photoluminescence measurements. The optical set-up scheme is represented in the Fig. S4 of the supporting information file (ESI†). A more detailed description of the components of the home built set-up can be found in the reference 68.

4. Conclusions

In conclusion, here we have shown a simple solution-based and low cost method of fabrication of nanowires with controlled and uniform size at room temperature. The process includes PDMS replica of DVD and CD profiles as substrates and it produces an array of aligned nanowires with a define width. We have applied this method to obtain all-inorganic lead halide $CsPbBr_3$ and hybrid $MAPbBr_3$

Con formato: Espacio Después: 4 pto

Perovskite nanowires starting from precursors solutions. However such procedure can be employed to achieve other material nanowires that can also be transferred to other suitable substrates.

The optical studies of all inorganic and hybrid lead Perovskite nanowires show the typical PL signal for these materials. Moreover, it can be excited at any point of the nanowire and guided along it towards its ends. Transport of light has been observed along the material for more than 12 μm. Experimental results are supported by theoretical simulation.

Acknowledgements

The authors would like to gratefully acknowledge financial support from Spanish Ministry of Economy and Competitiveness (MIMECO) (Severo Ochoa (SEV-2016-0683), MAT2015-69669-P projects) and Generalitat Valenciana (Prometeo II/2017/026 Excellency project). P.A. acknoledges the Fundación Ramón Areces (XVII Concurso Nacional para la adjudicación de Ayudas a la Investigación en Ciencias de la Vida y de la Materia) for its funding. F. R-M thanks the financial contribution of the Spanish Ministry of Economy and Competitiveness (MIMECO) through the program for young researchers support (TEC 2015 2015-74405-JIN). Finally, IR also thanks the Electron Microscopy Service of the Universitat Politècnica de València for their support in FESEM images acquisition and FIB milling, as well as Ana Moreno for her help in templates preparation.

Notes and references

1 Semiconductor nanowires: From next-generation Electronics to Sustainable Energy*; W.* Lu, J. Xiang, Eds; *RSC Smart Materials Series*, 2015
2 Semiconductor Nanowires, Materials, Synthesis, Characterization and Applications, J. Arbiol, Q. Xiong, Eds; Woodhead Publishing, 2015
3 K. Q. Peng, X. Wang, L. Li, Y. Hu, S.T. Lee, *Nano today*, 2013, **8**, 75
4 M. Mikolajick, W. M. Weber, Silicon Nanowires in Anisotropic Nanomaterials, Q. Li, Eds; Springer, 2015, pp.1-25
5 M. Hasan, M. F. Z. Huq, H. Mahmood, *Springer Plus,* 2013, **2**, 151
6 Z. Liu, Y. Mi, X. Guan, Z. Su, X. Liu, T. Wu, *Adv. Optical Mater.* 2018, **6**, 1800413
7 Y. Fu, H. Zhu, J. Chen, M. P. Hautzinger, X.-Y Zhu and S. Jin, Nature Reviews Materials, 2019, **4**, 169
8 J. S. Manser, J. A. Christians, P. V. Kamat, *Chem. Rev.* 2016, **116** (21), 12956
9 N. Kitazawa, Y. Watanabe, Y. Nakamura, *J. Mater. Sci.* 2002, **37**, 3585
10 J. Albero, H. Garcia, *J. Mater Chem.* C, 2017, **5**, 4098
11 G. Longo, M.-G. La-Placa, M. Sessolo, H. J. Bolink, *ChemSusChem*, 2017, **10**, 3788
12 J. M. Richter, M. Abdi-Jalebi, A. Sadhanala, M. Tabachnyk, J. P. H. Rivett, L. M. Pazos-Outón, K. C. Gödel, M. Price, F. Deschler, R. H. Friend, *Nature Comm.* 2016, **7**, 13941
13 F. Deschler, M. Price, S. Pathak, L. E. Klintberg, D.-D. Jarausch, R. Higler, S. Hüttner, T. Leijtens, S. D. Stranks, H. J. Snaith, M. Atatüre, R. T. Phillips, R. H. Friend, *J. Phys. Chem.,* 2014, **5**, 1421
14 S. De Wolf, J. Holvsky, S.-J. Moon, P. Löper, B. Niesen, M. Ledinsky, F.-J. Haug, J.-H. Yum, C. Ballif, *J. Phys. Chem. Lett*. 2014, **5**, 1035
15 C. Wehrenfennig, G. E. Eperon, M. B. Johnston, H. J. Snaith, L. M. Herz, *Adv. Mater.,* 2014, **26**, 1584
16 B. R. Sutherland, E. H. Sargent, *Nature Photonics*, 2016, **10**, 295
17 D. Bi, W. Tress, M. I. Dar, P. Gao, J. Luo, C. Renivier, K. Schenk, A. Abate, F. Giordano, J-P. Correa Baena, J.-D. Decoppet, S. M. Zakeeruddin, M. K. Nazeeruddin, M. Grätzel, A., *Sci. Adv.* 2016, **2** (1), e1501170
18 H. S. Jung, N-G. Park, *Small* 2015, **11** (1), 10-25
19 W. Zhang, G. E. Eperon, H. J. Snaith, *Nature Energy,* 2016, **1**, 16048
20 Y-H. Kim, C. Wolf, Y.-T. Kim, H. Cho, W. Kwon, S. Do, A. Sadhanala, C. G. Parl, S.-W. Rhee, S. H. Im, R. H. Friend, T.-W. Lee, *ACS Nano* 2017, **11**, 6586-6593
21 S. A. Veldhuis, P. P. Boix, N. Yantara, M. Li, T.C. Sum, N. Mathews, S. G. Mhaisalkar, Adv. Mater., 2016, **28**, 6804-6834
22 N. Wang, L. Cheng, R. Ge, S. Zhang, Y. Miao, W. Zou, C. Yi, Y. Sun, Y. Cao, R. Yang, Y. Wei, Q. Guo, Y. Ke, M. Yu, Y. Jin, Y. Liu, Q. Ding, D. Di, L. Yang, G. Xing, H. Tian, C. Jin, F. Gao, R. H. Friend, J. Wang, W. Huang, *Nature Photonics*, 2016, **10**, 699-704
23 H. Zhu, Y. Fu, F. Meng, X. Wu, Z. Gong, Q. Ding, M. V. Gustafsson, M. T. Trinh, S. Jin, X-Y. Zhu, *Nature Materials*, 2015, **14**, 636-642
24 J. R. Harwell, G. L. Whitworth, G. A. Turnbull, I. D. W. Samuel, *Scientific Reports*, 2017, **7**, 11727
25 Y. Jia, R. A. Kerner, A. J. Grede, B. P. Rand, N. C. Giebink, *Nature Photonics*, 2017, **11**, 784-788
26 G. Xing, N. Mathews, S. S. Lim, N. Yantara, X. Liu, D. Sabba, M. Gratzel, S. Mhaisalkar, T. C Sum, *Nature Materials*, 2014**,** **13**, 476-480
27 S. Zhang, P. Audebert, Y. Wei, A. Al Choueiry, G. Lanty, A. Bréhier, L. Galmiche, G. Clavier, C. Boissière, J.-S. Lauret, E. Deleporte, *Materials,* 2010, **3**, 3385-3406
28 M. Shoaib, X. Zhang, X. Wang, H. Zhou, T. Xu, X. Wang, X. Hu, H. Liu, X. Fan, W. Zheng, T. Yang, S. Yang, Q. Zhang, X. Zhu, L. Sun, A. Pan, *J. Am. Chem. Soc.,* 2017, **139**, 15592-15595-15595
29 J. Xing, X. F. Liu, Q. Zhang, S. T. Ha, Y. W. Yuan, C. Shen, T. C. Sum, Q. Xiong, *Nano Lett.*, 2015, **15** (7), 4571−4577.
30 L. Gu, M. M. Tavakoli, D. Zhang, Q. Zhang, A. Waleed, Y. Xiao, K.-H. Tsui, Y. Lin, L. Liao, J. Wang, Z. Fan, *Adv. Mater.,* 2016, **28** (44), 9713−9721.
31 Y. Wang, X Sun, R. Shivanna, Y. Yan, Z. Chen, Y. Guo, G-C. Wang, E. Wertz, F. Deschler, Z. Cai, H. Zhou, T-M. Lu, J. Shi, *Nano lett.,* 2016, **16**, 7974-7981.
32 K. Park, J. W. Lee, J. D. Kim, N. S. Han, D. M. Jang, S. Jeong, J. Park, J. K. J. Song, *Phys. Chem. Lett.*, 2016, **7** (18), 3703−3710
33 J. Chen, Y. Fu, L. Samad, L. Dang, Y. Zhao, S. Shen, L. Guo, S. Jin, *Nano Lett.*, 2017, **17**, 460-466
34 H. Zhou, S. Yuan, X. Wang, T. Xu, X. Wang, H. Li, W. Zheng, P. Fan, Y. Li, L. sun, A. Pan, *ACS Nano*, 2017, **11** (2) 1189-1195
35 X. Wang, H. Zhou, S. Yuan, W. Zheng, Y. Jiang, X. Zhuang, H. Liu, Q. Zhang, X. Zhu, X. Wang, A. Pan, *Nano Research*, 2017, **10** (10), 3385-3395

36 E. Oksenberg, E. Sanders, R. Popovitz-Biro, L. Houben, E. Joselevich, *Nanolett.*, 2018, **18** (1), 424-433
37 J. Chen, Z. Luo, Y. Fu, X. Wang, K. J. Czech, S. Shen, L. Guo, J. C. Wright, A. Pan and S. Jin, *ACS Energy Lett*., 2019, **4** (5), 1045
38 S. W. Eaton, M. Lai, N.A. Gibson, A. B. Wong, L. Dou, J. Ma, L-W Wang, S. R. Leone, P. Yang, *PNAS,* 2016, **113**, 8, 1993-1998
39 M. M. Tavakoli, A. Waleed, L. Gu, D. Zhang, R.Tavakoli, B. Lei, W. Su, F. Fang, Z. Fan, *Nanoscale,* 2017, **9** (18), 5828–5834
40 J.-H. Im, J. Luo, M. Franckevičius, N. Pellet, P. Gao, T. Moehl, S. M. Zakeeruddin, M. K. Nazeeruddin, M. Grätzel, N.-G. Park, *Nano Lett.,* 2015, **15** (3), 2120–2126
41 A. B. Wong, M. Lai, S. W. Eaton, Y. Yu, E. Lin, L. Dou, A. Fu, P. Yang, *Nano Lett.*, 2015, **15** (8), 5519–5524
42 H. Deng, D. Dong, K. Qiao, L. Bu, B. Li, D.Yang, H.-E.Wang, Y. Cheng, Z. Zhao, J. Tang, H. Song, *Nanoscale*, 2015, **7** (9), 4163–4170.
43 M. Spina, E. Bonvin, A. Sienkiewicz, B. Náfradi, L. Forró, E. Horváth, *Sci. Rep.,* 2016, **6** (1), 19834
44 M. J. Ashley, M. N. O'Brien, K. R. Hedderick, J. A. Mason, M. B. Ross, C. A. Mirkin, *J. Am. Chem. Soc.,* 2016, **138** (32), 10096–10099
45 W. Deng, L. Huang, X. Xu, X. Zhang, X. Jin, S.-T. Lee, J. Jie, *Nano Lett.*, 2017, **17** (4), 2482–2489
46 S. Wang, K. Wang, Z. Gu, Y. Wang, C. Huang, N. Yi, S. Xiao, Q. Song, *Adv. Optical Mater.*, 2017, **5**, 1700023.
47 A. A. Petrov, N. Pellet, J.-Y. Seo, N. A. Belich, D. Y. Kovalev, A. V. Shevelkov, E. A. Goodilin, S. M. Zakeeruddin, A. B.Tarasov, M. Graetzel, *Chem. Mater.,* 2017, **29** (2), 587–594
48 Y. Fu, H. Zhu, C. C. Stoumpos, Q. Ding, J. Wang, M. G. Kanatzidis, X. Zhu, S. Jin, *ACS Nano,* 2016, **10** (8), 7963-7972.
49 D. Zhang, S. W. Eaton, Y. Yu, L. Dou, P. Yang, *J. Am. Chem. Soc.,* 2015, **137**, 9230-9233
50 D. Zhang, Y. Yang, Y. Bekenstein, Y. Yu, N. A. Gibson, A. B. Wong, S. W. Eaton, N. Kornienko, Q. Kong, M. Lai, A. P. Alivisatos, S. R. Leone, P. Yang, *J. Am. Chem. Soc.,* 2016, **138**, 13155-13158
51 Y. Fu, H. Zhu, A. W. Schrader, D. Liang, Q. Ding, P. Joshi, L. Hwang, X-Y. Zhu, S. Jin, *Nano Lett.*, 2016, 16, 1000-1008
52 P. Liu, X. He, J. Ren, Q. Liao, J. Yao, H. Fu, *ACS Nano,* 2017, **11**, 5766-5773
53 M. M. Lee, J. Teuscher, T. Miyasaka, T. N. Murakami, H. J. Snaith, *Science,* 2012, **338**, 643-647
54 G. Niu, X. Guo, L. Wang, *J. Mater. Chem. A*, 2015, **3**, 8970
55 T. A Berhe, W.-N. Su, C.-H. Chen, C.-J. Pan, J.-H. Cheng, H. –M. Chen, M.-C. Tsai, L.-Y. Chen, A. A. Dubale, B.-J. Hwang, *Energy Environ. Sci.,* 2016, **9**, 323
56 B. Brunetti, C. Cavallo, A. Ciccioli, G. Gigli, A. Latini, *Scientific Reports,* 2016, **6**, 31896
57 B. Conings, J. Drijkoningen, N. Gauquelin, A. Babayigit, J. D'Haen, L. D'Oliestlaeger, A. Ethirajan, J. Verbeeck, J. Manca, E. Mosconi, F. De Angelis, H. -G. Boyen, *Adv. Energy Mater.,* 2015, **5**, 1500477
58 M. Kulbak, S. Gupta, N. Kedem, I. Levine, T. Bendikov, G. Hodes, D. Cahen, J. *Phys. Chem. Lett.*, 2016, **7**, 167-172
59 M. Saliba, T. Matsui, J-Y. Seo, K. Domanski, J-P Correa Baena, M. K. Nazeeruddin, S. M. Zakeeruddin, W. Tresss, A. Abate, A. Hagfeldt, M. Gratzel, *Energy Environ. Sci.,* 2016, **9**, 1989-1997
60 R. F. Service, *Science,* 2016, **351**, 113-114
61 J. Kang, L.W. Wang, *J. Phys. Chem. Lett.,* 2017, **8**, (2) 489-493
62 Y. Wang, X. Sun, R. Shivanna, Y. Yang, Z. Chen, Y. Guo, G-C Wang, E. Wertz, F. Deschler, Z. Cai, H. Zhou, T-M. Lu, J. Shi, *NanoLett.,* 2016, **16**, 7974-7981
63 L. M. Pazos-Outón, M. Szumilo, R. Lamboll, J. M. Richter, M. Crespo-Quesada, M. Abdi-Jalebi, H. J. Beeson, M. Vruéinié, M. Alsari, H. J. Snaith, B. Ehrler, R. H. Friend, F. Deschler, *Science*, 2016, **351** (6280), 1430-1433
64 I. Dursun, Y. Zheng, T. Guo, M. De Bastiani, B. Turedi, L. Sinatra, Md A. Haque, B. Sun, A. A. Zhumekenov, M. I. Saidaminov, F. P. Garcia de Arquer, E. H. Sargent, T. Wu, Y. N. Garstein, O. M. Bakr, O. F. Mohammed, A. V. Malko, *ACS Energy Lett.,* 2018, **3**, 1492-1498
65 F. Ramiro-Manzano, R. García-Aboal, R. Fenollosa, S. Basi, I. Rodriguez, P. Atienzar, F. Meseguer, Optical properties of organic/inorganic perovskite microcrystals through the characterization of Fabry-Pérot resonances. 2019, submitted
66 F. Ramiro-Manzano, E. Bonnet, I. Rodriguez, F. Meseguer, *Langmuir,* 2010, **26** (7), 4559-4562.
67 R. García-Aboal, R. Fenollosa, F. Ramiro-Manzano, I. Rodriguez, F. Meseguer, P. Atienzar, *ACS Omega* 2018, **3**, 5229-5236
68 R. Fenollosa M. Garín, F. Meseguer, *Phys. Rev. B,* 2016, **93**, 235307